

Neurons Merging Layer: Towards Progressive Redundancy Reduction for Deep Supervised Hashing

Chaoyou Fu^{1234*} Liangchen Song^{4*} Xiang Wu¹² Guoli Wang⁴ Ran He^{123†}

¹ Center for Research on Intelligent Perception and Computing, CASIA

² National Laboratory of Pattern Recognition, CASIA

³ University of Chinese Academy of Sciences

⁴ Horizon Robotics

{chaoyou.fu, rhe}@nlpr.ia.ac.cn, alfredxiangwu@gmail.com
{liangchen.song, guoli.wang}@horizon.ai

Abstract

Deep supervised hashing has become an active topic in web search and information retrieval. It generates hashing bits by the output neurons of a deep hashing network. During binary discretization, there often exists much redundancy among hashing bits that degenerates retrieval performance in terms of both storage and accuracy. This paper formulates the redundancy problem in deep supervised hashing as a graph learning problem and proposes a novel layer, named Neurons Merging Layer (NMLayer). The NMLayer constructs a graph to model the adjacency relationship among different neurons. Specifically, it learns the relationship by the defined active and frozen phases. According to the learned relationship, the NMLayer merges the redundant neurons together to balance the importance of each output neuron. Based on the NMLayer, we further propose a progressive optimization strategy for training a deep hashing network. That is, multiple NMLayers are progressively trained to learn a more compact hashing code from a long redundant code. Extensive experiments on four datasets demonstrate that our proposed method outperforms state-of-the-art hashing methods.

Introduction

With the explosive growth of data, hashing has been one of the most efficient indexing techniques and drawn substantial attention (Lai et al. 2015). Hashing aims to map high dimensional data into a binary low-dimension Hamming space. Equipped with the binary representation, hashing can be performed with constant or sub-linear computation complexity, as well as the markedly reduced space complexity (Gong and Lazebnik 2011). Traditionally, the binary hashing codes can be generated by random projection (Gionis, Indyk, and Motwani 1999) or learned from data distribution (Gong and Lazebnik 2011).

Over the last few years, inspired by the remarkable success of deep learning, researchers have paid much attention to combining hashing with deep learning (Xia et al. 2014; Cao et al. 2016). Particularly, by utilizing the similarity information for supervised learning, deep supervised hashing has greatly improved the performance of hashing retrieval

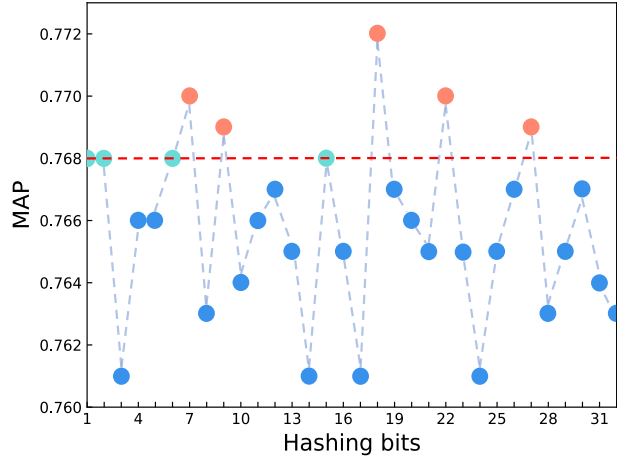


Figure 1: Illustration of the redundancy in hashing bits generated by a common CNN-F network (Chatfield et al. 2014). The horizontal red dotted line represents the mean average precision (MAP) calculated using all bits. The vertical axis represents the Mean Average Precision calculated after removing corresponding bit. For example, removing the 1-st bit does not affect the MAP, while removing the 3-nd bit leads to a remarkable drop of MAP. Even more, the MAP increases after removing the 18-th bit.

(Li, Wang, and Kang 2016; Jiang and Li 2018). In general, the last layer of a neural network is modified as the output layer of hashing bits. Then, both features and hashing bits are learned from the neural network during optimizing the hashing loss function, which is elaborately designed to keep the similarities among the input data.

Despite the effectiveness of the existing deep supervised hashing methods, the redundancy of hashing bits remains a problem that has not been well studied (Lai et al. 2015; Du et al. 2018). As shown in Figure 1, we can see that the redundancy has a significant impact on the retrieval performance. Because of the redundancy, the importance of different hashing bits varies greatly. However, a straightforward intuition is that all hashing bits should be equally important. In order to address the redundancy problem, we propose a simple yet effective method to balance the importance of each bit in the hashing codes. In details, we pro-

*Equal contribution

†Corresponding author

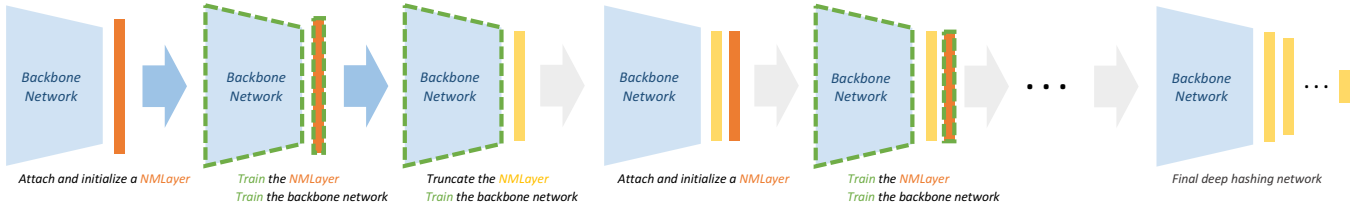


Figure 2: Illustration of our progressive optimization strategy. For a standard backbone network, i.e., deep hashing network, we first attach and initialize a NMLayer after the hashing layer. Then, we train the NMLayer as well as the backbone network for a certain number of epochs. Next, based on the learned adjacency relationship among neurons, the NMLayer is truncated to determine which neurons to merge. After that, according to the truncation results, we continue to train the backbone network. At this point, the training process of the first NMLayer is completed. By iterating the above process, which is attaching NMLayer and optimizing the whole network, we finally get the required hashing bits. Note that although many NMLayers are attached, total weights of the network change little. Because each time completing the training of a NMLayer, we just determine which neurons in the hashing layer to merge, without adding extra weights.

pose a new layer named Neurons Merging Layer (NMLayer) for deep hashing networks. It constructs a graph to model the adjacency relationship among different neurons. During the training process, the NMLayer learns the relationship by the defined active and frozen phases, as shown in Figure 3. Through the learned relationship, the NMLayer dynamically merges the redundant neurons together to balance the importance of each neuron. In addition, by training multiple NMLayers, we propose a progressive optimization strategy to gradually reduce the redundancy. The full process of our progressive optimization strategy is illustrated in Figure 2. Extensive experimental results on the CIFAR-10, NUS-WIDE, MS-COCO and Clothing1M (in appendix) datasets verify the effectiveness of our method. In short, our main contributions are summed up as follows:

1. We formulate the redundancy problem as a graph learning problem, and propose a mechanism that consists of the active and frozen phases to effectively learn the adjacency relationship. This graph results in a new layer named NMLayer, which reduces the redundancy of hashing bits by balancing the importance of each bit. The NMLayer can be easily integrated into a standard deep neural network.
2. We design a progressive optimization strategy for training deep hashing networks. A deep hashing network is initialized with more hashing bits than the required bits, then the redundancy is progressively reduced by multiple NMLayers that form a graph learning. Compared with other hashing methods of fixed code length, NMLayers obtain a more compact code from a redundant long code.
3. Extensive experimental results on four challenging datasets show that our proposed method achieves significant improvements, when compared with state-of-the-art hashing methods.

Related Work

Hashing for Image Retrieval

Existing hashing methods can be grouped into two categories, i.e., data-independent hashing methods and data-dependent hashing methods. In data-independent hashing methods,

hashing functions are mostly defined by random projection or manually constructed, e.g., locality sensitive hashing (LSH) (Gionis, Indyk, and Motwani 1999). Compared with data-dependent hashing methods, data-independent hashing methods are usually incapable of generating compact hashing codes on the short coding length (Jiang and Li 2018). In recent years, most hashing algorithms are designed in data-dependent manner.

Generally, the training data is utilized in two different aspects in data-dependent methods, including unsupervised and supervised way. Representative unsupervised hashing methods include iterative quantization hashing (ITQ) (Gong and Lazebnik 2011) and ordinal embedding hashing (OEH) (Liu et al. 2016b). Both of them explore the metric structure among the training data and thus retrieve the neighbors. Though learning in an unsupervised manner avoids the demand of the annotated data, exploiting the available supervisory information usually implies a better hashing code. For instance, supervised hashing with kernels (KSH) (Liu et al. 2012) employs a kernel function to optimize the Hamming distance of data pairs. Other supervised hashing methods based on hand-crafted features, including latent factor hashing (LFH) (Zhang et al. 2014) and column-sampling based discrete supervised hashing (COSDISH) (Kang, Li, and Zhou 2016), also exhibit impressive results.

Moreover, benefit from deep neural networks, deep supervised hashing methods have made great progress (Xia et al. 2014; Cao et al. 2016; Mu and Liu 2017; Lin, Li, and Tang 2017; Wang et al. 2018; Xu et al. 2018). Convolutional neural network hashing (CNHN) (Xia et al. 2014) is one of the early deep supervised hashing methods, which learns features and hashing codes in two separate stages. On the contrary, deep pairwise-supervised hashing (DPSH) (Li, Wang, and Kang 2016) integrates the feature learning stage and hashing optimization stage in an end-to-end framework. In addition, some works (Lai et al. 2015; Guo et al. 2018) utilize multiple sub-models to learn different bits to reduce the relevance among hashing bits. However, as far as we know, no work has been done to specifically study and address the redundancy problem in deep supervised hashing.

Network Redundancy Reducing

Reducing the redundancy of neural networks is a well studied topic. Some early works can date back to (Mozer and Smolensky 1989; LeCun, Denker, and Solla 1990), in which they remove the least relevant units in a network. More recently, (Liu et al. 2015) removes entire neurons based on the idea that neurons have little influence on the output of the network should be removed. Similarly, in (Yu et al. 2018), they measure the importance of neurons in the final response layer and propose Neuron Importance Score Propagation to propagate the importance to every neuron in the network. Although these methods take the saliency of individual parameters or neurons into consideration, they zero out parameters or neurons in the network to reduce the number of parameters complexity. However, by and large, our problem setting is finding out the redundancy in output hashing bits and thus merging the output neurons to achieve a better performance when compared with the network that contains same hashing bits. A more related work is (Du et al. 2018), in which they notice the redundancy of hashing bits when using an unsupervised generative method and then reduce the redundancy by adding a constraint in the loss function. In addition, a non-deep supervised hashing method (Jiang and Li 2015) learns the hashing function in a bit-wise manner. By sequentially learning hashing bits, the residual caused by former bits can be reduced.

Preliminaries and Notations

Notation

We use uppercase letters like A to denote matrices and use a_{ij} to denote the (i, j) -th element in matrix A . The transpose of A is denoted by A^\top . $\text{sgn}(\cdot)$ is used to denote the element wise sign function, which returns 1 if the element is positive and returns -1 otherwise.

Problem Definition

Suppose we have n images denoted as $X = \{x_i\}_{i=1}^n$, where x_i denotes the i -th image. Furthermore, the pairwise supervisory similarity is denoted as $S = \{s_{ij}\}$. $s_{ij} \in \{-1, +1\}$, where $s_{ij} = -1$ means x_i and x_j are dissimilar images and $s_{ij} = +1$ means x_i and x_j are similar images.

Deep supervised hashing aims at learning a binary code $b_i \in \{-1, +1\}^K$ for each image x_i , where K is the length of binary codes. $B = \{b_i\}_{i=1}^n$ denotes the set of all hashing codes. The Hamming distance $\text{dist}_H(b_i, b_j) = 0.5 \times (K - b_i^\top b_j)$ of the learned binary codes of image x_i and x_j should keep consistent with the similarity attribute s_{ij} . That is, similar images should have shorter Hamming distances, while dissimilar images should have longer Hamming distances.

Neurons Merging Layer

In this section, we describe the details of NMLayer, which aims at balancing the importance of each hashing output neuron. A NMLayer has two phases during the training process, namely the active phase and the frozen phase, as shown in Figure 3. Basically, when a NMLayer is initially attached after a hashing output layer, it is set in the active phase to

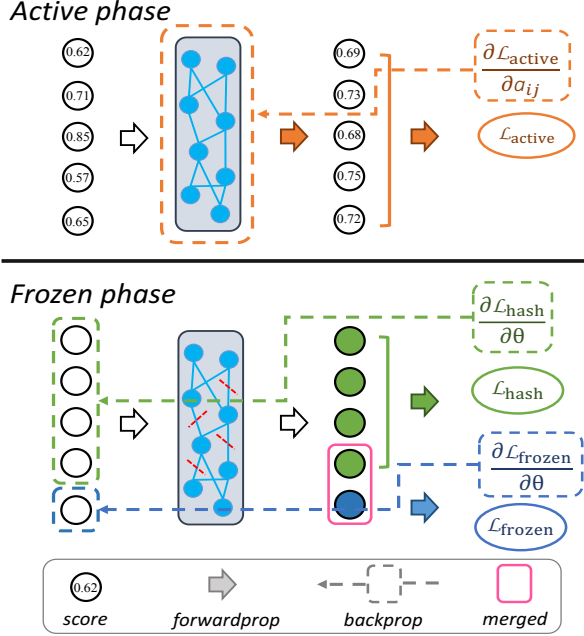


Figure 3: Illustration of the two phases of our NMLayer. In the active phase, we calculate the score of each neuron and then utilize the active loss (Eq. (3)) to update the adjacency relationship, i.e., the adjacency matrix. In the frozen phase, after truncating the adjacency matrix, the hashing loss and the frozen loss (Eq. (5)) are used to update corresponding neurons.

learn the adjacency relationship, i.e., the adjacency matrix, among different hashing bits. After enough updating on the weights through backpropagation, we truncate the adjacency matrix to determine which neurons to merge. Then, the NMLayer is set to frozen phase to learn hashing bits. The above process can be iterated for several times until the final output of the network reaches the required hashing bits. Actually, the learning process of a NMLayer is constructing a graph G . The neurons of a NMLayer are nodes, while the adjacency matrix A denotes the set of all edges. In the remainder of this section, we begin with presenting the basic structure of the NMLayer and then introduce the different policies of forward and backward in the active and frozen phases. Next, we define the behavior of the NMLayer when the neural network is in the evaluation mode. Finally, we introduce our progressive optimization strategy in detail.

Structure of the NMLayer

As mentioned above, a NMLayer is basically a graph G with learnable adjacency matrix A . Note that G is an undirected graph, i.e., $a_{ij} = a_{ji}$. The nodes of G are denoted by \mathcal{V} , which is a set of hashing bits. Specifically, the value type of A differs in two phases. During the active phase, A is learned through backpropagation and $A \in \mathbb{R}^{|\mathcal{V}| \times |\mathcal{V}|}$, where $|\mathcal{V}|$ means the number of nodes. Each element in A denotes the necessity whether the two nodes should be merged as one single node. After entering frozen phase, the graph structure

is fixed, that is A becomes fixed and now $A \in \{0, 1\}^{|\mathcal{V}| \times |\mathcal{V}|}$, where $a_{ij} = 1$ means that the i -th and j -th neurons are merged, while $a_{ij} = 0$ means the opposite.

Active Phase

When a NMLayer is first attached and initialized, all the elements in A are set to 0, which indicates that no nodes are currently merged or inclined to be merged. In the active phase, our target is to find out which nodes should be merged together, based on a simple intuition that all nodes, i.e., all hashing bits, should carry equal information about the input data. In our NMLayer, the principle is restated in a practical way that eliminating any single hashing bit should lead to an equal decline of performance, thus no redundancy in the final hashing bits. Next, we elaborate on how to evaluate the importance of neurons in a typical forward pass of neural networks.

Forward. Suppose the size of a mini-batch in a forward pass is N , the number of neurons are K , and the neurons are $\{v_1, \dots, v_K\}$. In each forward pass, scores that evaluating the importance of each neuron are computed for the next backward pass. More precisely, for each neuron we compute the retrieval precision, i.e., mean average precision (MAP), after eliminating it. We denote the input of the mini-batch as $\{X_n\}_{n=1}^N$ and the validation set as \mathcal{Y} , then the score s_k of the k -th neuron is computed as

$$s_k = \text{Prec}_k(X_n, \mathcal{Y}), \quad (1)$$

where the function $\text{Prec}(X_n, \mathcal{Y})$ means computing the precision with query \mathcal{Y} and gallery X_n , and the subscript k means computing precision without the k -th hashing bit. Recall that in the active phase, elements in A imply the necessity of whether two nodes in the graph should be merged. In the forward pass, we take A into consideration to calculate new scores $\{s'_k\}_{k=1}^K$, that is

$$s'_i = s_i + \frac{1}{2}a_{ij}(s_j - s_i). \quad (2)$$

The intuition of the above equation is that if s_i and s_j are merged together, i.e., $a_{ij} = 1$, then s'_i is equal to s'_j . Next, we update A according to the $\{s'_k\}_{k=1}^K$ in the following backward pass.

Backward. In order to update A through backpropagation, a loss function $\mathcal{L}_{\text{active}}$ is defined on $\{s'_k\}_{k=1}^K$. The principle of the loss function is to determine the inequality among neurons. Therefore, a feasible and straightforward loss function is

$$\mathcal{L}_{\text{active}} = \sum_{i \neq j} |s'_i - s'_j|. \quad (3)$$

In fact, by Eq. (3), the partial derivative of $\mathcal{L}_{\text{active}}$ with respect to a_{ij} is

$$\frac{\partial \mathcal{L}_{\text{active}}}{\partial a_{ij}} = \text{sgn}(s'_i - s'_j) \cdot (s_j - s_i). \quad (4)$$

Observing that, due to the utilized $L1$ loss in Eq. (3), the value of derivative depends on $s_j - s_i$. It can be interpreted that the more different two nodes are, the higher necessity the two nodes should be merged.

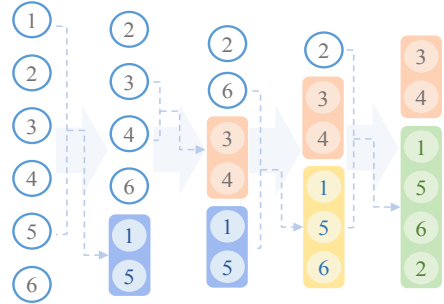


Figure 4: A demonstration of the merging process from six neurons to two neurons. At each step, we merge two neurons.

Truncation of the Adjacency Matrix

With A being updated for several epochs, we then perform a truncation on A to merge neurons. After truncating A , all the elements in A are either 0 or 1. Nodes with an adjacency value of 1 will be merged, and output new hashing bits with other nodes. Similar to the choice of loss function $\mathcal{L}_{\text{active}}$, the strategy of truncation is various and we just use a straightforward one. We turn the maximum m values in A to 1, and the others to 0.

Frozen Phase

If all the values of matrix A are 0, that is the NMLayer neither trained nor truncated, both of the forward pass and backward pass are the same as a normal neural network. When some elements in A are 1, it means the corresponding neurons are merged together. The new node that consists of the merged nodes has new forward and backward strategies. We illustrate our strategy with a simple case. Suppose that two nodes $\{v_1, v_2\}$ are merged together, i.e., $a_{12} = 1$. Therefore, the length of the output hashing bits is now $K - 1$, and we denote the new node as v_{12} , then the new output hashing bits are $\{v_{12}, v_3, \dots, v_K\}$.

Forward. We randomly choose one node from the new merged node as the output in the forward pass. Note that, choosing a random node or a fixed order node as the output has little impact on the retrieval result, which is demonstrated in our supplementary material. In our simple example, v_1 is randomly chosen and the output of v_{12} is equal to v_1 . Moreover, if v_1 and v_2 are also merged nodes and contain several neurons respectively, we randomly choose one neuron from all neurons as the output.

Backward. For the node chosen for output, the gradient in the backward pass is simply calculated by the loss of hashing networks, such as a pairwise hashing loss like Eq. (7). As for those nodes not chosen in the new merged node, we set a target according to the sign of the chosen output node. In our simple example, the gradient of v_1 is calculated according to the pairwise hashing loss, and the loss of v_2 is computed by $\|v_2 - \text{sgn}(v_1)\|^2$. The intuition that not directly using the same gradient as v_1 is to reduce the correlation among the

Algorithm 1: Progressively training multiple Neural Merging Layers.

```

input : Training set  $X$ , validation set  $\mathcal{Y}$ , initial hashing bits  $B_{\text{in}}$ , truncation parameter  $m$ , iteration number  $N_0, N_1$ .
output: The network with hashing bits  $B_{\text{out}}$  .
1 Initialize the backbone network  $F^{(1)}$  ;
2 for  $t = 1, \dots, T$  do
3   Attach NMLayer  $G^{(t)}$  after  $F^{(t)}$ :
4    $F^{(t)} \leftarrow F^{(t)} + G^{(t)}$  ;
5   Set  $G^{(t)}$  in the active phase;
6   for  $i = 1, \dots, N_0$  do
7     | Train  $F^{(t)}$  by Eq. (3), Eq. (7);
8   end
9   Truncate  $G^{(t)}$  ;
10  Set  $G^{(t)}$  in the frozen phase;
11  for  $j = 1, \dots, N_1$  do
12    | Train  $F^{(t)}$  by Eq. (5), Eq. (7);
13  end
14 end

```

neurons. More generally, for all of the neurons in the new merged node expect the neuron v_j chosen in the forward pass, the loss function is defined as

$$\mathcal{L}_{\text{frozen}} = \sum_{i \neq j} \|v_i - \text{sgn}(v_j)\|^2. \quad (5)$$

Evaluation Mode

When the whole network is set in evaluation mode, we no longer choose the output of a merged node in a random manner. Instead, we compute the output of the merged node by majority-voting. Again, using the simple example above, the output of v_{12} depends on $\text{sgn}(v_1)$ and $\text{sgn}(v_2)$. That is, if $\text{sgn}(v_1) = \text{sgn}(v_2) = +1$ then $v_{12} = +1$. Note that when $\text{sgn}(v_1) = +1$ and $\text{sgn}(v_2) = -1$, then $v_{12} = 0$, which implies that the output of v_{12} is uncertain. In this paper, we directly calculate the Hamming distance without especially considering this particular case and leave this study for our future pursuit.

Progressive Optimization Strategy

By training multiple NMLayers progressively, we merge the output neurons of a deep hashing network as shown in Figure 2. Meanwhile, the detailed algorithm is shown in Algorithm 1. Note that we use multiple NMLayers instead of one because the redundancy is reduced by gradually merging neurons. Merging too many neurons at once will degrade algorithm performance, which is reported in our supplemental material. By performing the algorithm, we aim to get a network with B_{out} hashing bits from a backbone network F with B_{in} hashing bits. Hyper-parameters in the algorithm are shown as follow: m means turning the maximum m values of the adjacency matrix to 1 and the others to 0, which is defined in the truncation operation; the active phase and frozen

phase are trained by N_0 and N_1 epochs respectively. For better understanding, we show a simple example in Figure 4, in which we have 6 output hashing neurons at the beginning and merge 2 neurons per step.

Experiments

In this section, we begin with the implementation details, in which the pairwise hashing loss is mathematically described and parameters are given. Then, we analyze the potential redundancy in hashing bits, which is the key motivation of our NMLayer. Next, in order to show the effectiveness of our proposed method, we conduct a series of comparative experiments. Finally, we compare our method with state-of-the-art hashing methods. Note that, other experiments like more detailed experimental analysis and parameter discussion are reported in our supplemental material.

Implementation Details

Pairwise Hashing Loss. Following the optimization method of (Liu et al. 2012), we maintain the similarity s_{ij} between images x_i and x_j by optimizing the inner product of b_i and b_j :

$$\begin{aligned} \min_B \quad & \mathcal{L}_{\text{hash}} = \sum_{i=1}^m \sum_{j=1}^n (b_i^\top b_j - ks_{ij})^2 \\ \text{s.t.} \quad & b_i, b_j \in \{-1, +1\} \end{aligned} \quad (6)$$

where m and n are the number of query images and retrieval images respectively. However, solving Eq. (6) is a discrete optimization problem, which is difficult to directly optimize. Note that for the input image x_i , the output of our neural network is denoted by $u_i = F(x_i, \theta)$ (θ is the parameter of our neural network), and the binary hashing code b_i is equal to $\text{sgn}(u_i)$. In order to solve the discrete optimization problem, we replace the binary code b_i with u_i and add a L_2 regularization term as (Li, Wang, and Kang 2016), then the reformulated loss function can be written as

$$\begin{aligned} \min_{U, \Theta} \quad & \mathcal{L}_{\text{hash}} = \sum_{i=1}^m \sum_{j=1}^n (u_i^\top u_j - ks_{ij})^2 + \eta \sum_{i=1}^n \|b_i - u_i\|_2^2 \\ \text{s.t.} \quad & u_i, u_j \in \mathbb{R}^{k \times 1}, b_i = \text{sgn}(u_i) \end{aligned} \quad (7)$$

where η is a hyper-parameter and Eq. (7) is used as our basic pairwise hashing loss.

Parameter Settings. The CNN-F network (Chatfield et al. 2014) is widely used in deep supervised hashing (Li, Wang, and Kang 2016; Li et al. 2017; Zhu and Gao 2017; Jiang and Li 2018), which contains five convolutional layers and three fully connected layers. Therefore, for fair comparison with previous methods, we adopt the CNN-F network pre-trained on the ImageNet dataset (Russakovsky et al. 2015) as the backbone of our method. The last fully connected layer of the CNN-F network is modified to hashing layer. The parameters in our algorithm are experimentally set as follows. Note that the effects of the parameters B_{in} and m are reported in the supplemental material. The number of neurons in the hashing layer is set to 60, which is

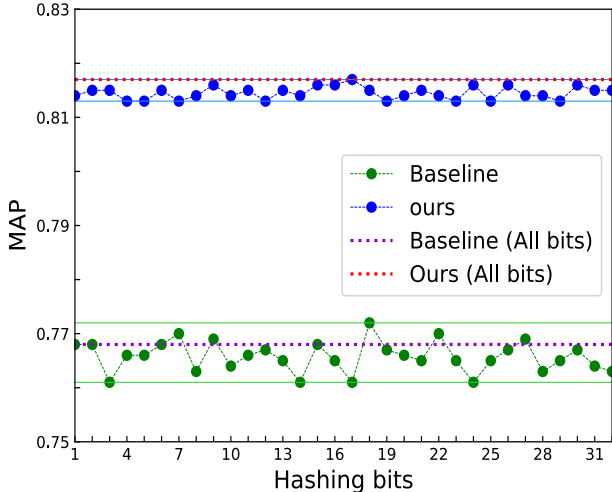


Figure 5: The redundancy reduction of hashing bits by our algorithm.

B_{in} in our algorithm. The number of truncating edges in per step, i.e. m , is set to 4. During training, we set the batch size to 128 and use stochastic gradient descent (SGD) with 10^{-4} learning rate and 10^{-5} weight decay to optimize the backbone network. In addition, the learning rate of NMLayer and the hyper-parameter η in Eq. (7) are set to 10^{-2} and 1200 respectively. Moreover, the parameters N_0 and N_1 are set to 5 and 40 respectively.

Datasets and Evaluation Methodology

Datasets. The CIFAR-10 dataset (Krizhevsky and Hinton 2009) contains 60,000 images. It is a single-label dataset. The division of our query set and database set are same with (Li, Wang, and Kang 2016). In addition, because we need a validation set to calculate the score of neurons, we randomly select 200 images from the training set as our validation set and use the rest 4,800 images as our training set.

The NUS-WIDE dataset (Chua et al. 2009) contains 269,648 images. It is a multi-label dataset in which each image belongs to multiple classes. Our query set and database set are same with (Li, Wang, and Kang 2016). Moreover, we randomly divide the training set into 420 images and 10,080 images as our validation set and training set respectively.

The MS-COCO dataset (Lin et al. 2014b) contains 82,783 training images. It is also a multi-label dataset. The division of our query set and database set are same with (Jiang and Li 2018). Then, 400 images are randomly selected from the training set as our validation set and the rest 9,600 images are used as our training set.

The Clothing1M dataset (Xiao et al. 2015) is a large-scale dataset that contains 1,037,497 images. The detailed data division is reported in the supplemental material.

For the single-label CIFAR-10 dataset, images with the same label are considered to be similar ($s_{ij} = 1$). For the multi-label NUS-WIDE and MS-COCO datasets, two images are considered to be similar ($s_{ij} = 1$) if they share at least one common label.

Evaluation Methodology. We use Mean Average Precision (MAP) to evaluate the retrieval performance. Specially, the MAP of the NUS-WIDE dataset is calculated based on the top 5,000 returned samples. In addition, in order to make a fair comparison, the training set of the compared hashing methods is the sum of our validation set and training set.

Analyses of Redundancy in Hashing Bits

On the CIFAR-10 dataset, we utilize Eq. (7) to train a 32 bits hashing network without NMLayer as *Baseline* method. Then, in order to show the redundancy of hashing bits, we remove a bit per time and report the final MAP with our method and the baseline method in Figure 5. From Figure 5 we can clearly observe that the variance of MAP among the hashing bits is much lower in our algorithm, thus we can come to the conclusion that the redundancy in hashing bits has been indeed reduced. In addition, as the redundancy is reduced, each bit of hashing codes can be fully utilized. Therefore, the retrieval precision is greatly improved. In the supplemental material, we further present and analyze the change of MAP during gradually reducing the hashing bit from 60 to 1.

Comparison with Other Variants

In order to further verify the effectiveness of our method, we elaborately design several variants of our method, which are straightforward solutions towards the reduction of redundancy. Firstly, considering that the dropout technique (Srivastava et al. 2014) is widely adopted in neural networks to reduce the correlation among neurons, we add a dropout layer before the hashing layer to reduce the correlation of hashing bits and denote it as *Dropout*. Secondly, we design a variant that has multiple randomly assigned neurons for each hashing bit and denote it by *Random*. This variant is equal to replacing the learning of the adjacency matrix in the active phase with random assignment and using our frozen phase strategy at the same time. Finally, since the process of our neurons merging can be viewed as a process of dimension reduction, we also compare the differences between our NMLayer and the fully connected layer. This variant with fully connected layer is denoted by *FCLayer*. Specially, we add a 32 bits fully connected layer after our 60 bits hashing layer as the new hashing layer, which is optimized by loss function Eq. (7). Meanwhile, the 60 bits hashing layer is turned to a normal fully connected layer.

The above variants are compared using three evaluation metrics as (Xia et al. 2014): Precision-Recall curves, Precision curves within Hamming distance 2, and Precision curves with different numbers of top returned samples. The results of above variants are reported in Figure 6. From Figure 6 we can see that the improvement of *Dropout* and *FCLayer* over *Baseline* is small, which proves the effects of the dropout technique and the fully connected layer are limited to the hashing retrieval. Meanwhile, *Random* achieves better results than *Dropout* and *FCLayer*, which demonstrates the effectiveness of our frozen phase. More importantly, our method outperforms all other variants by a large margin.

Table 1: MAP of different methods on the CIFAR-10, NUS-WIDE and MS-COCO datasets. The results on the large-scale Clothing1M dataset are reported in the supplemental material.

Method	CIFAR-10				NUS-WIDE				MS-COCO			
	12 bits	24 bits	32 bits	48 bits	12 bits	24 bits	32 bits	48 bits	12 bits	24 bits	32 bits	48 bits
Ours	0.786	0.813	0.821	0.828	0.801	0.824	0.832	0.840	0.754	0.772	0.777	0.782
LCDSH	0.752	0.794	0.801	0.810	0.776	0.803	0.810	0.819	N/A	N/A	N/A	N/A
DSDH	0.740	0.786	0.801	0.820	0.776	0.808	0.820	0.829	N/A	N/A	N/A	N/A
DPSH	0.713	0.727	0.744	0.757	0.775	0.801	0.807	0.818	0.746	0.766	0.772	0.777
DSH	0.644	0.742	0.770	0.799	0.712	0.731	0.740	0.748	0.696	0.717	0.715	0.722
DHN	0.680	0.721	0.723	0.733	0.771	0.801	0.805	0.814	0.744	0.765	0.769	0.774
COSDISH	0.583	0.661	0.680	0.701	0.642	0.740	0.784	0.796	0.689	0.692	0.731	0.758
SDH	0.453	0.633	0.651	0.660	0.764	0.799	0.801	0.812	0.695	0.707	0.711	0.716
FastH	0.597	0.663	0.684	0.702	0.726	0.769	0.781	0.803	0.719	0.747	0.754	0.760
LFH	0.417	0.573	0.641	0.692	0.711	0.768	0.794	0.813	0.708	0.738	0.758	0.772
ITQ	0.261	0.275	0.286	0.294	0.714	0.736	0.745	0.755	0.633	0.632	0.630	0.633

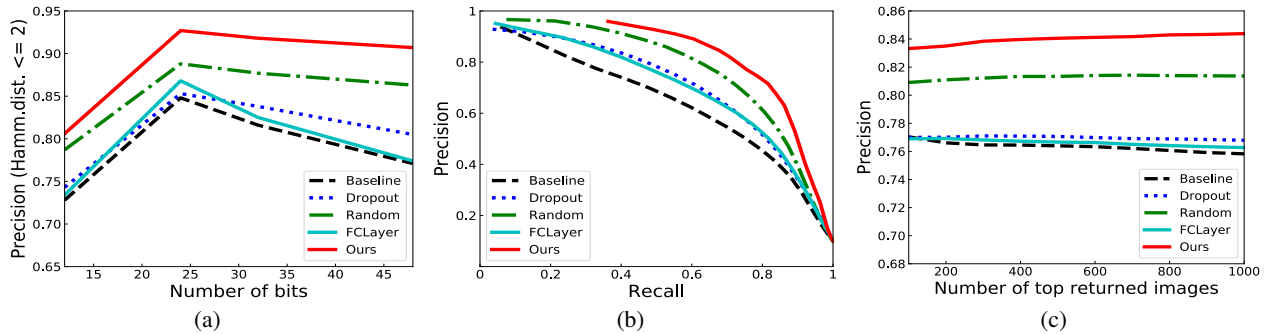


Figure 6: The comparison results on the CIFAR-10 dataset. (a) precision curves within Hamming distance 2; (b) precision-recall curves of Hamming ranking with 32 bits; (c) precision curves with 32 bits w.r.t. different numbers of top returned samples.

Comparison with State-of-the-art Methods

We compare our method with several state-of-the-art hashing methods, including one unsupervised method iterative quantization hashing (ITQ) (Gong and Lazebnik 2011); four non-deep supervised methods, column-sampling based discrete supervised hashing (COSDISH) (Kang, Li, and Zhou 2016), supervised discrete hashing (SDH) (Shen et al. 2015), fast supervised hashing (FastH) (Lin et al. 2014a), latent factor hashing (LFH) (Zhang et al. 2014); five deep supervised methods, locality constrained deep supervised hashing (LCDSH) (Zhu and Gao 2017), deep supervised discrete hashing (DSDH) (Li et al. 2017), deep pairwise-supervised hashing (DPSH) (Li, Wang, and Kang 2016), deep supervised hashing (DSH) (Liu et al. 2016a), and deep hashing network (DHN) (Zhu et al. 2016). Note that other methods like network in network hashing (NINH) (Lai et al. 2015) are not compared in our experiments, because they have been outperformed by the compared methods like DPSH.

In Table 1, the MAP results of all methods on the CIFAR-10, NUS-WIDE and MS-COCO datasets are reported. For fair comparison, most of the results are directly reported from previous works (Li et al. 2017; Zhu and Gao 2017; Jiang and Li 2018). Particularly, the results of DPSH on the NUS-WIDE dataset come from re-running the released code. Note that some results are not reported because the

authors neither perform experiment on the corresponding dataset nor release their complete source code. As we can see from Table 1, compared with the unsupervised hashing method, the supervised methods achieve better results in most cases. Meanwhile, in all supervised hashing methods, the deep hashing methods outperform the non-deep hashing methods. Furthermore, our method outperforms all other hashing methods on all datasets, which validates the effectiveness of our method.

Conclusion

In this paper, we analyze the redundancy of hashing bits in deep supervised hashing. To address this, we formulate the redundancy problem as a graph learning problem and propose a novel layer named NMLayer. The NMLayer merges the redundant neurons together to balance the importance of each hashing bit. Moreover, based on the NMLayer, we propose a progressive optimization strategy. A deep hashing network is initialized with more hashing bits than the required bits, and then multiple NMLayers are progressively trained to learn a more compact hashing code from a redundant long code. Our approach is highly effective, which is verified by different experimental results on four datasets.

References

Cao, Y.; Long, M.; Wang, J.; Zhu, H.; and Wen, Q. 2016. Deep quantization network for efficient image retrieval. In *AAAI*.

Chatfield, K.; Simonyan, K.; Vedaldi, A.; and Zisserman, A. 2014. Return of the devil in the details: Delving deep into convolutional nets. In *BMVC*.

Chua, T.-S.; Tang, J.; Hong, R.; Li, H.; Luo, Z.; and Zheng, Y. 2009. Nus-wide: a real-world web image database from national university of singapore. In *CIVR*.

Du, C.; Xie, X.; Du, C.; and Wang, H. 2018. Redundancy-resistant generative hashing for image retrieval. In *IJCAI*.

Gionis, A.; Indyk, P.; and Motwani, R. 1999. Similarity search in high dimensions via hashing. In *VLDB*.

Gong, Y., and Lazebnik, S. 2011. Iterative quantization: A procrustean approach to learning binary codes. In *CVPR*.

Guo, Y.; Zhao, X.; Ding, G.; and Han, J. 2018. On trivial solution and high correlation problems in deep supervised hashing. In *AAAI*.

Jiang, Q.-Y., and Li, W.-J. 2015. Scalable graph hashing with feature transformation. In *IJCAI*.

Jiang, Q.-Y., and Li, W.-J. 2018. Asymmetric deep supervised hashing. In *AAAI*.

Kang, W.-C.; Li, W.-J.; and Zhou, Z.-H. 2016. Column sampling based discrete supervised hashing. In *AAAI*.

Krizhevsky, A., and Hinton, G. 2009. Learning multiple layers of features from tiny images. *Master's thesis, University of Toronto*.

Lai, H.; Pan, Y.; Liu, Y.; and Yan, S. 2015. Simultaneous feature learning and hash coding with deep neural networks. In *CVPR*.

LeCun, Y.; Denker, J. S.; and Solla, S. A. 1990. Optimal brain damage. In *NIPS*.

Li, Q.; Sun, Z.; He, R.; and Tan, T. 2017. Deep supervised discrete hashing. In *NIPS*.

Li, W.-J.; Wang, S.; and Kang, W.-C. 2016. Feature learning based deep supervised hashing with pairwise labels. In *IJCAI*.

Lin, G.; Shen, C.; Shi, Q.; Van den Hengel, A.; and Suter, D. 2014a. Fast supervised hashing with decision trees for high-dimensional data. In *CVPR*.

Lin, T.-Y.; Maire, M.; Belongie, S.; Hays, J.; Perona, P.; Ramanan, D.; Dollár, P.; and Zitnick, C. L. 2014b. Microsoft coco: Common objects in context. In *ECCV*.

Lin, J.; Li, Z.; and Tang, J. 2017. Discriminative deep hashing for scalable face image retrieval. In *IJCAI*.

Liu, W.; Wang, J.; Ji, R.; Jiang, Y.-G.; and Chang, S.-F. 2012. Supervised hashing with kernels. In *CVPR*.

Liu, B.; Wang, M.; Foroosh, H.; Tappen, M. F.; and Pensky, M. 2015. Sparse convolutional neural networks. In *CVPR*.

Liu, H.; Wang, R.; Shan, S.; and Chen, X. 2016a. Deep supervised hashing for fast image retrieval. In *CVPR*.

Liu, H.; Ji, R.; Wu, Y.; and Liu, W. 2016b. Towards optimal binary code learning via ordinal embedding. In *AAAI*.

Mozer, M. C., and Smolensky, P. 1989. Skeletonization: A technique for trimming the fat from a network via relevance assessment. In *NIPS*.

Mu, Y., and Liu, Z. 2017. Deep hashing: A joint approach for image signature learning. In *AAAI*.

Russakovsky, O.; Deng, J.; Su, H.; Krause, J.; Satheesh, S.; Ma, S.; Huang, Z.; Karpathy, A.; Khosla, A.; Bernstein, M.; Berg, A. C.; and Fei-Fei, L. 2015. Imagenet large scale visual recognition challenge. *IJCV* 115(3):211–252.

Shen, F.; Shen, C.; Liu, W.; and Tao Shen, H. 2015. Supervised discrete hashing. In *CVPR*.

Srivastava, N.; Hinton, G.; Krizhevsky, A.; Sutskever, I.; and Salakhutdinov, R. 2014. Dropout: a simple way to prevent neural networks from overfitting. *JMLR* 15(1):1929–1958.

Wang, D.; Huang, H.; Lu, C.; Feng, B.-S.; Nie, L.; Wen, G.; and Mao, X.-L. 2018. Supervised deep hashing for hierarchical labeled data. In *AAAI*.

Xia, R.; Pan, Y.; Lai, H.; Liu, C.; and Yan, S. 2014. Supervised hashing for image retrieval via image representation learning. In *AAAI*.

Xiao, T.; Xia, T.; Yang, Y.; Huang, C.; and Wang, X. 2015. Learning from massive noisy labeled data for image classification. In *CVPR*.

Xu, P.; Huang, Y.; Yuan, T.; Pang, K.; Song, Y.-Z.; Xiang, T.; Hospedales, T. M.; Ma, Z.; and Guo, J. 2018. Sketchmate: Deep hashing for million-scale human sketch retrieval. In *CVPR*.

Yu, R.; Li, A.; Chen, C.-F.; Lai, J.-H.; Morariu, V. I.; Han, X.; Gao, M.; Lin, C.-Y.; and Davis, L. S. 2018. Nisp: Pruning networks using neuron importance score propagation. In *CVPR*.

Zhang, P.; Zhang, W.; Li, W.-J.; and Guo, M. 2014. Supervised hashing with latent factor models. In *SIGIR*.

Zhu, H., and Gao, S. 2017. Locality-constrained deep supervised hashing for image retrieval. In *IJCAI*.

Zhu, H.; Long, M.; Wang, J.; and Cao, Y. 2016. Deep hashing network for efficient similarity retrieval. In *AAAI*.

Supplemental Material

In this material, we conduct a series of supplementary experiments to further prove the effectiveness of our method. First, we present and analyze the change of MAP during progressively reducing the hashing bit from 60 to 1. Next, we show the effects of our proposed random node selection manner in the frozen phase, as well as the sensitivity with respect to the hyper-parameters B_{in} and m . Then, we compare our method with other state-of-the-art algorithms under the same number of parameters. Finally, we further validate the performance of our method on a large-scale dataset.

Bit Reduction

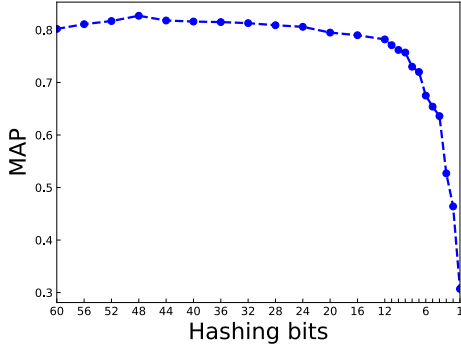


Figure 1: MAP results during progressively reducing the hashing bit from 60 to 1 on the CIFAR-10 dataset.

We set the parameters B_{in} and m to 60 and 4 respectively. In order to more precisely analyze the retrieval accuracy during the bit reduction process, we reduce m to 1 when the bit number is less than 12. The curve of accuracy change is presented in Figure 1. As we can see from Figure 1, the MAP value increases from 60 bits to 48 bits. This is due to the effective redundancy reduction of our approach, through which each bit can be fully utilized. In addition, we can see that the 48 bits can achieve the best retrieval performance. Therefore, we consider 48 as the most appropriate code length on the CIFAR-10 dataset. Inspired by this insight, our approach can also be conducive to finding the most appropriate code length while reducing the redundancy. Moreover, observing that the MAP value drops slowly from 48 bits to 7 bits, and when the code length decreases to 6, the MAP value drops significantly. Hence, the minimum code length to provide precise retrieval accuracy is 7. In addition, we note that when the code length is less than 4, it is no longer able to provide enough information for retrieval.

Sensitivity to Parameters

Figure 2 (a) presents the results of the node selection in the frozen phase. In the new merged node, we respectively select the first, second and random neurons as our output in the forward pass. From Figure 2 (a) we can see that choosing which neuron as the output has less impact on the MAP. In addition, Figure 2 (b) and Figure 2 (c) present the effects of hyper-parameters B_{in} and m , which denote the number of initial neurons in the hashing layer and the number of truncating edge per step respectively. From Figure 2 (b) and Figure 2 (c) we find that our approach is not sensitive to these parameters in a large range, which validates the robustness of our method. Note that increasing the number of B_{in} dose not improve the retrieval accuracy, it may due to that 60 bits already have enough expression capacity and more neurons are saturated. In addition, the retrieval results decrease when m is too large, which demonstrates that merging too many neurons at once will degrade the performance of our algorithm. This is the reason why we use multiple NMLayers to gradually merge neurons.

Table 1: MAP of different methods on the CIFAR-10, NUS-WIDE and MS-COCO datasets with the same parameters. The best results for each category are shown in boldface.

Method	CIFAR-10				NUS-WIDE				MS-COCO			
	12 bits	24 bits	32 bits	48 bits	12 bits	24 bits	32 bits	48 bits	12 bits	24 bits	32 bits	48 bits
Ours	0.750	0.797	0.813	0.825	0.774	0.812	0.827	0.832	0.744	0.769	0.775	0.780
LCDSH	0.752	0.794	0.801	0.810	0.776	0.803	0.810	0.819	N/A	N/A	N/A	N/A
DSDH	0.740	0.786	0.801	0.820	0.776	0.808	0.820	0.829	N/A	N/A	N/A	N/A
DPSH	0.713	0.727	0.744	0.757	0.775	0.801	0.807	0.818	0.746	0.766	0.772	0.777
DSH	0.644	0.742	0.770	0.799	0.712	0.731	0.740	0.748	0.696	0.717	0.715	0.722
DHN	0.680	0.721	0.723	0.733	0.771	0.801	0.805	0.814	0.744	0.765	0.769	0.774
COSDISH	0.583	0.661	0.680	0.701	0.642	0.740	0.784	0.796	0.689	0.692	0.731	0.758
SDH	0.453	0.633	0.651	0.660	0.764	0.799	0.801	0.812	0.695	0.707	0.711	0.716
FastH	0.597	0.663	0.684	0.702	0.726	0.769	0.781	0.803	0.719	0.747	0.754	0.760
LFH	0.417	0.573	0.641	0.692	0.711	0.768	0.794	0.813	0.708	0.738	0.758	0.772
ITQ	0.261	0.275	0.286	0.294	0.714	0.736	0.745	0.755	0.633	0.632	0.630	0.633

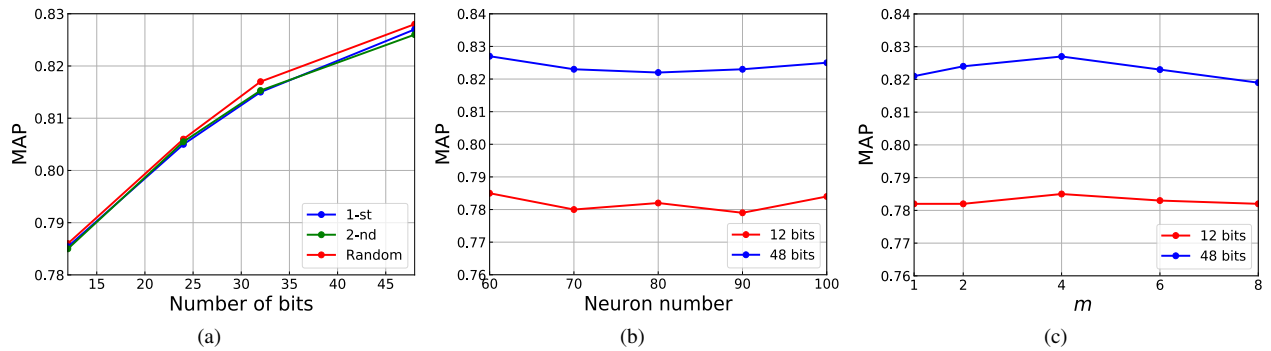


Figure 2: Parameter analysis experiments on the CIFAR-10 dataset. (a) Different node selection strategy comparison; (b) Sensitivity analysis with respect to parameter B_{in} ; (c) Sensitivity analysis with respect to parameter m .

Comparison under Same Number of Parameters

In order to further demonstrate the effectiveness of redundancy reduction, we set the number of initial neurons of hashing layer to 12, 24, 32 and 48 respectively, then we reduce the redundancy of these hashing bits by our method. We record the best MAP value in the process of bit reduction and compare it with state-of-the-art hashing methods, which is reported in Table 1. As for 12 bits, due to the short code length, the redundancy is low. Therefore, the results of our method are slightly worse than state-of-the-art methods, like DPSH. However, our method is still superior to all other hashing methods in the 24, 32 and 48 bits.

Experiments on the Large-scale Dataset

The Clothing1M dataset is a large-scale dataset that contains 1,037,497 images. It is a single-label dataset. The division of our query set (7,000 images) and database set (about 1,020,000 images) are same with [1]. In addition, 280 images are randomly selected from the training set as our validation set and the rest 13,720 images are used as our training set.

On the Clothing1M dataset, we compare our method with deep discrete supervised hashing (DDSH) [1] and other state-of-the-art hashing methods. The results are reported in Table 2. Note that the results of compared methods come from [1]. From Table 2 we can see that our method outperforms all state-of-the-art methods on the Clothing1M dataset.

Table 2: MAP of different methods on the Clothing1M dataset. The best results for each category are shown in boldface.

Method	Clothing1M			
	12 bits	24 bits	32 bits	48 bits
Ours	0.311	0.372	0.389	0.401
DDSH	0.276	0.366	0.387	0.400
DSDH	0.290	0.328	0.341	0.347
DPSH	0.195	0.208	0.216	0.218
DSH	0.173	0.187	0.191	0.202
DHN	0.190	0.224	0.212	0.248
COSDISH	0.187	0.235	0.256	0.275
SDH	0.151	0.186	0.194	0.197
FastH	0.173	0.206	0.216	0.244
LFH	0.154	0.159	0.212	0.257
ITQ	0.083	0.089	0.091	0.092

References

[1] Qing-Yuan Jiang, Xue Cui, and Wu-Jun Li. Deep discrete supervised hashing. *TIP*, 27(12):5996–6009, 2018.